

A comparison of singlet and triplet states for one- and two-dimensional graphene nanoribbons using multireference theory

Shawn Horn · Felix Plasser · Thomas Müller ·
Florian Libisch · Joachim Burgdörfer ·
Hans Lischka

Received: 31 January 2014 / Accepted: 22 May 2014
© Springer-Verlag Berlin Heidelberg 2014

Abstract This study examines the radical nature and spin symmetry of the ground state of the quasi-linear acene and two-dimensional periacene series. For this purpose, high-level ab initio calculations have been performed using the multireference averaged quadratic coupled cluster theory and the COLUMBUS program package. A reference space consisting of restricted and complete active spaces is taken for the π -conjugated space, correlating 16 electrons with 16 orbitals with the most pronounced open-shell character for the acenes and a complete active-space reference approach

with eight electrons in eight orbitals for the periacenes. This reference space is used to construct the total configuration space by means of single and double excitations. By comparison with more extended calculations, it is shown that a focus on the π space with a 6-31G basis set is sufficient to describe the major features of the electronic character of these compounds. The present findings suggest that the ground state is a singlet for the smaller members of these series, but that for the larger ones, singlet and triplet states are quasi-degenerate. Both the acenes and periacenes exhibit significant polyradical character beyond the traditional diradical.

Dedicated to the memory of Professor Isaiah Shavitt and published as part of the special collection of articles celebrating his many contributions.

Electronic supplementary material The online version of this article (doi:10.1007/s00214-014-1511-8) contains supplementary material, which is available to authorized users.

Keywords Singlet–triplet splitting · MR-AQCC · Unpaired electron density · Natural orbitals

S. Horn · H. Lischka (✉)
Department of Chemistry and Biochemistry, Texas Tech
University, Lubbock, TX 79409-1061, USA
e-mail: hans.lischka@univie.ac.at

F. Plasser
Interdisciplinary Center for Scientific Computing,
Ruprecht-Karls-University, Im Neuenheimer Feld 368,
69120 Heidelberg, Germany

T. Müller
Institute of Advanced Simulation, Jülich Supercomputer Centre,
Forschungszentrum Jülich, 52425 Jülich, Germany

F. Libisch · J. Burgdörfer
Institute for Theoretical Physics, Vienna University of
Technology, Wiedner Hauptstrasse 8–10, 1040 Vienna, Austria

H. Lischka
Institute for Theoretical Chemistry, University of Vienna,
Währingerstrasse 17, 1090 Vienna, Austria

1 Introduction

Over the past decade, there has been significant rise in graphene research due to its potential application in nanoelectronics [1] and organic semiconductors [2]. This enthusiasm was triggered by the so-called scotch tape isolation [3] performed in 2004 by Geim and Novoselov. After isolating a one-atom-thick sheet of graphite, which they would coin as “graphene,” many experimental and theoretical groups began to explore the peculiar electronic properties of this zero-bandgap semiconductor [4]. Quasi-linear acenes (Fig. 1a) and two-dimensional nanoribbons [5] (Fig. 1b) have been frequently used to investigate the fascinating electronic properties of graphene. The synthesis of quasi-linear n -acenes is possible up to 9-acene, but beyond 5-acene, measures must be taken to overcome its high reactivity. For hexacene, emersion in silicone oil solution has been used by Ref. [6]. Heptacene has been

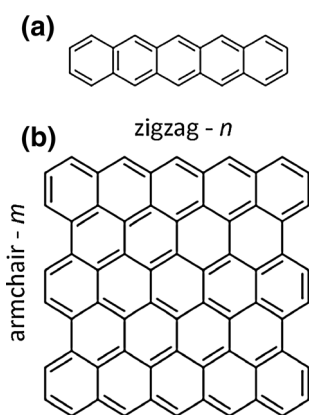


Fig. 1 Structures **a** n -acene and **b** (m, n) periacene

photogenerated in a polymethyl methacrylate matrix [7]. Octacene and nonacene were kept at very low temperatures (~ 30 K) in a solid argon matrix by Tonshoff and Bettinger [8]. Additionally, although not preserving the true molecules, significant substitution by bulky groups has been used to stabilize the acenes [9].

Extensive theoretical work has been performed on acenes [10–13] and graphene flakes [14–18] using density functional theory (DFT) calculations. However, because of the polyradical character of these systems, an unrestricted approach had to be used [10] with concomitant spin contamination, demonstrating the energetic instability of the restricted DFT procedure [11]. Furthering this, Scuseria et al. [12] used a spin-projected UHF (SUHF) to overcome the deficiencies in a standard single-determinant HF approach. As an alternative, the density matrix renormalization group (DMRG) [19, 20] and the active-space variational two-electron reduced density matrix (2-RDM) methods [21, 22] aim at an exact solution within a full configuration space spanned by a limited basis set (minimal or non-polarized double zeta basis sets) in the π space. The spin-flip configuration interaction method [23] and coupled cluster with singles, doubles, and non-iterative triples CCSD(T) [24, 25] have been applied as well. Recently, multireference averaged quadratic coupled cluster (MR-AQCC) calculations [26], with all σ molecular orbitals (MOs) frozen, have been performed.

The extraordinary spin polarization and half-metallic properties of zigzag graphene nanoribbons (GRN) (Fig. 1) [5] have been demonstrated in many investigations based on general considerations using Clar's sextet theory [27, 28] and by explicit quantum chemical calculations using DFT [14, 16, 18, 29], DMRG [19, 20], 2-RDM [21, 22], and MR-AQCC methods [26]. Singlet–triplet (S-T) splitting gives important information about the radical character of a compound. It was first estimated by Angliker et al. [6] that the ground state of nonacene and beyond was a triplet

state. This estimate was based on the extrapolation of the experimentally observed singlet–triplet splitting available between benzene and pentacene to nonacene. But in 2010, Tonshoff and Bettinger [8] concluded from the existence of a finite optical band gap deduced from Vis/NIR spectroscopy that nonacene was in fact a singlet, while, e.g., in [30], EPR spectra for substituted nonacene were observed indicating a non-singlet state. Additionally, several theoretical groups [19, 31–33] report S-T splittings for acenes and S–S excitation energies have been examined as well [34]. For a detailed discussion on these findings, see Sect. 3.

The present study explores the spin symmetry and radical nature of graphene nanoribbons via quasi-linear acenes as well as two-dimensional periacenes. There are two questions this study seeks to answer: (1) What is the spin state of the ground state of acenes and periacenes, and can this knowledge then be used to extrapolate this to a larger graphene nanoribbon? (2) What can be said about the radical nature of graphene?

The first question posed is addressed with calculations using multiconfigurational and multireference ab initio methods. Multireference averaged quadratic coupled cluster (MR-AQCC) [35] calculations are particularly useful for large aromatic systems and radical systems [26, 36, 37], of which the molecules in this study are both. This approach aims at a compact representation of complicated electronic wave functions by constructing a reference space containing the most important quasi-degenerate configurations (non-dynamical electron correlation) and representing the dynamical correlation by means of single and double excitations [38]. Size extensivity contributions are taken care of by the AQCC approach. To answer the second question, an analysis of the radical nature of the acenes is performed by two means: tracking the evolution of both the natural orbital (NO) occupations with increasing chain length and the total number of effectively unpaired electrons (N_U). The method for determining N_U was first proposed by Takatsuka et al. [39] and was further developed by Staroverov and Davidson [40]. The methodology eventually used in this paper comes from Head-Gordon [41]. Additionally, we investigate the influence of freezing the σ orbitals on the NO occupations and the S-T splittings. The effect of polarized basis sets on these quantities is considered as well.

2 Computational methods

For the purposes of this study, the “zigzag” edge of the acenes and periacenes is taken to be along the x -axis in the x - y plane. The acenes were examined from $n = 2$ –13, n being the number of fused benzene rings in the chain.

The periacenes were studied from $(5a,2z)$ to $(5a,5z)$, in which m and n count the number of benzene rings along each direction and a and z denote armchair and zigzag boundaries, respectively (Fig. 1b). These molecules belong to the D_{2h} symmetry group, with b_{1u} , b_{2g} , b_{3g} , a_u being the irreducible representations that correspond to the π orbitals. The geometries for the acenes and periacenes were taken from Ref. [26], which had been optimized with second-order Møller–Plesset perturbation theory [42] including the resolution of the identity approach (RI-MP2) [43, 44] with an SV(P) basis set [45] under D_{2h} symmetry.

As a first option in constructing the multireference wave function, a complete active-space (CAS) approach was chosen. In this, eight electrons were correlated with eight orbitals (two taken from each π symmetry). This resulting CAS(8,8), although modified at times, was used throughout the calculations of the periacenes. CAS self-consistent field (CASSCF) calculations were performed to determine the MOs. This CAS(8,8) was used as a reference space in constructing a multireference (MR) expansion in configuration state functions (CSF) with all single and double excitations [38]. This MR expansion was used in two ways. The multireference averaged quadratic coupled cluster (MR-AQCC) method [35] is our preferred method in the reliable treatment of static and dynamic electron correlation effects. In calculations of higher triplet states, which were performed to determine the symmetry of the lowest one, the MR-AQCC method suffered from the problem of intruder states. In these cases, and for the purpose of comparison with MR-AQCC calculations on the lowest triplet state, the multireference configuration interaction with singles and doubles (MR-CISD) method was employed, also using the same configuration space as for the MR-AQCC approach. To account for quadruple and higher excitations, the renormalized Davidson correction [38, 46] (denoted + Q) was used as follows:

$$E_Q = \frac{(1 - c_0^2)(E_{CI} - E_{SCF})}{c_0^2} \quad (1)$$

in which c_0^2 is the sum of the squared coefficients of the reference configurations in the MR-CISD expansion.

We found that the periacenes were well described by the MR-AQCC/CAS(8,8) approach. In the case of the larger members of the n -acene series (n larger than 8), a significant number of intruder states appeared. This resulted in configurations (mostly singly excited either from the doubly occupied orbitals into the CAS or from the CAS to the virtual orbital space) not included in the references. Configurations exceeding a threshold of 0.01 in their weight in the CSF expansion were considered intruder states. Moreover, in such cases, the reference space was not preserved throughout the calculations. Consequently, the symmetry

numbering of the output natural orbitals (NOs) did not correspond to that of the MOs used for the construction of the reference space in the input. We therefore set up an extended scheme as second option, in which the number of internal orbitals was significantly increased. However, including these orbitals as a CAS proved to be too costly. Following the procedures used by Plasser et al. [26], a set of active orbitals was introduced by moving some reference doubly occupied orbitals into the restricted active space (RAS) from which only single excitations were allowed in the process of constructing the references. Similarly, auxiliary orbitals were introduced by moving virtual orbitals into the auxiliary active space (AUX). Only a single electron, at most, was permitted into the AUX. The set of reference CSFs constructed from this RAS/CAS/AUX scheme was then used to construct the entire CSF expansion space by means of single and double excitations as described above for the CAS(8,8) reference space.

The RAS is composed of orbitals that are generally in the $1.84e$ – $1.90e$ range for NO occupation. The number of RAS orbitals used for $n = 2$ – 6 was n , and for $n = 7$ – 13 , six orbitals were maintained as in the 6-acene. Their contribution to the reference space is greater than that of the doubly occupied space, but less than that of the CAS. Based on experience with the calculations on the singlet state of the n -acenes [26], a CAS(4,4) was taken for all n , correlating 4 electrons with 4 orbitals. These orbitals exhibited the most pronounced open-shell character in the CAS(8,8) calculation. They are, therefore, given the largest weight in the reference space. The range of their NO occupation is from $0.25e$ to $1.75e$. The auxiliary space (AUX) is the excitation space for the reference configurations. The AUX orbitals generally have an NO occupation of $0.07e$ – $0.15e$.

This calculation is referred to as RAS/CAS(4,4)/AUX in the following. A total of 16 electrons/orbitals are used, at most, in this reference space, as opposed to the 8 in the CAS(8,8) reference space. This RAS/CAS(4,4)/AUX representation is used at the MCSCF, MR-CISD, and MR-AQCC levels. For the n -acenes, $n = 9$ – 11 , one additional configuration was added to the reference space to accommodate for a significant intruder state in the MR-AQCC wave function.

In terms of molecular size, the most extended set of calculations were performed by freezing all σ orbitals and using the 6-31G basis set [47]. Starting from a closed-shell self-consistent field (SCF) calculation, all occupied and virtual σ orbitals were frozen by transforming the one- and two-electron integrals into a new basis, keeping only the π orbitals. The effect of the frozen σ orbitals was folded into effective one-electron Hamilton matrix elements according to the formalism described by Shavitt [48]. To validate the use of the 6-31G basis set and the freezing of σ orbitals,

two additional sets of calculations were performed for the n -acenes up to $n = 9$. The first was identical to the scheme outlined above, except a 6-31G* basis set [47] was used. The second series of calculations also used a 6-31G* basis set, but froze only the σ core orbitals. In these calculations though, a smaller reference space was chosen. For $n = 2-4$, a CAS(4,4) was sufficient as a reference space, which is the same CAS(4,4) as in the RAS/CAS(4,4)/AUX. For $n = 5$, one orbital was added to both the RAS and the AUX space based on their proximity to CAS occupations. For $n = 6-7$, two RAS and AUX orbitals were added, and an additional amount of σ orbitals equal to the number of 1s core orbitals was frozen. This procedure was tested for $n = 7$, and no significant deviation in S-T splitting energies was found. This second calculation was only used up to $n = 7$.

The effective unpaired electron densities and total number of effectively unpaired electrons (N_U) were computed [39–41]. To avoid overemphasizing the contribution of the natural orbitals (NOs) that are nearly occupied or nearly unoccupied, we chose to use the nonlinear model suggested in [41] where N_U is given by

$$N_U = \sum_{i=1}^M n_i^2 (2 - n_i)^2 \quad (2)$$

in which n_i is the occupation of the i th NO and M is the number of NOs. In this, the open-shell character is given the largest weight.

The orbital occupation scheme of the doubly occupied orbitals was obtained by performing a DFT calculation with the Becke–Perdew functional [49, 50] and a 6-31G* basis set [47]. Geometry optimizations were performed with the TURBOMOLE [51, 52] package, and all other calculations use COLUMBUS [53–55].

3 Results

3.1 Singlet–triplet splitting

A direct product of all the π symmetries for D_{2h} results in the following symmetries for the triplet states: 3A_g , ${}^3B_{3u}$, ${}^3B_{2u}$, and ${}^3B_{1g}$. The S-T splitting for the π -MR-CISD + Q/CAS(8,8)/6-31G calculation for each of these symmetries (i.e., the excitation energies from the 1^1A_g state to the respective lowest triplet state in these symmetries) is compared in order to determine the lowest energy state. It is shown in Figs. 2 and 3 (Tables S1–2 in the Supplementary Material contain the data in tabular form; the same procedure has been followed for the other figures showing S-T splittings) that the ${}^3B_{3u}$ state has the smallest S-T splitting for all molecules. In light of this,

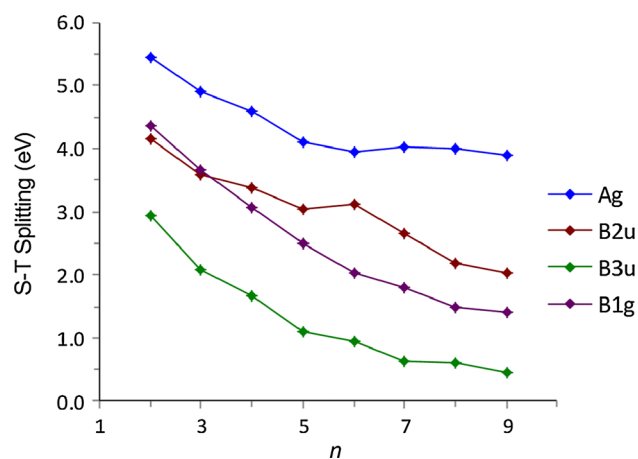


Fig. 2 Singlet–triplet splitting of n -acenes ($n = 2-9$) with respect to the 1^1A_g ground state using the π -MR-CISD + Q/CAS(8,8)/6-31G approach

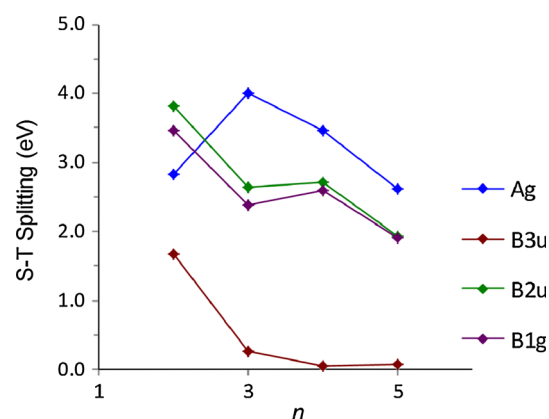


Fig. 3 Singlet–triplet splitting of ($5a,nz$) periacenes ($n = 2-5$) with respect to the 1^1A_g ground state using the π -MR-CISD + Q/CAS(8,8)/6-31G approach

only the ${}^3B_{3u}$ symmetry was considered in the remaining work.

The S-T splitting for the MCSCF, MR-CISD, and MR-AQCC calculations for the acenes (Fig. 4, Table S3) remains positive in all instances, indicating that the system maintains singlet ground state character for these computational levels and all values of n investigated. However, the relative theoretical–experimental error, as shown in Table 1, shows that the π -MR-AQCC/RAS/CAS(4,4)/AUX/6-31G results deviate by 0.27 ± 0.06 eV from the experimental data [31, 56–59]. Correcting our results by this value shows that our calculations predict 11-acene as the first case where the triplet state is lower than the singlet state, as it can be seen from S-T splitting of 0.26 in Table S3. This value of $n = 11$ compares quite well with the value of $n = 9$ deduced by Angliker et al. [6] from

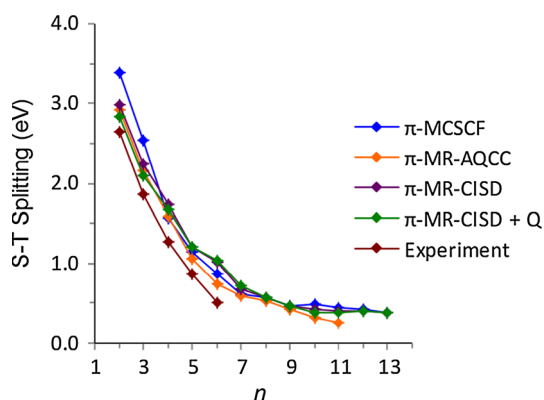


Fig. 4 Singlet–triplet splitting for n -acenes ($n = 2$ –13) at four different levels of theory using a π -RAS/CAS(4,4)/AUX reference space and the 6-31G basis set in comparison with experimental data

Table 1 Average difference and standard deviation of the S-T splitting (eV) between theory and experiment for the linear acenes $n = 2$ –6

Method	Average \pm standard deviation
π -MCSCF/6-31G	0.48 ± 0.22
π -MCSCF/6-31G*	0.48 ± 0.18
Total-MCSCF/6-31G*	0.70 ± 0.13
π -MR-CISD/6-31G	0.41 ± 0.06
π -MR-CISD + Q/6-31G	0.33 ± 0.13
π -MR-AQCC/6-31G	0.27 ± 0.05
π -MR-AQCC/6-31G*	0.29 ± 0.08
Total-MR-AQCC/6-31G*	0.40 ± 0.19

experimental data as mentioned above. The difference between these two n values comes from a slight leveling off of the MR-AQCC results (Fig. 4).

π -MR-CISD/6-31G and π -MR-CISD + Q/6-31G calculations have been performed for $n = 12$ and 13 with the present RAS/CAS/AUX scheme, for which the MR-AQCC calculation showed significant intruder states. It is interesting to note that until $n = 10$, the former two methods as well as MCSCF show very good agreement with the MR-AQCC data, and only starting at $n = 10$, no further reduction of the S-T splitting is observed for these methods. This good agreement with the MR-AQCC reference data is partly due to the flexible reference configuration set, but probably also due to error cancelation in computing the energy difference between singlet and triplet states.

While it is possible that acenes maintain a singlet ground state as n approaches infinity, they surely have nearly degenerate singlet and triplet ground states. A similar situation is present in the much larger periacene system, in which the S-T splitting, as shown in Fig. 5

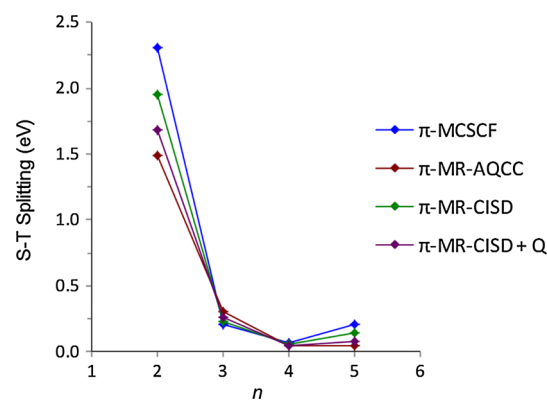


Fig. 5 Singlet–triplet splitting for $(5a, n_z)$ periacenes ($n = 2$ –5) at four different levels of theory with the σ system frozen using a CAS(8,8) reference configuration set

(Table S4), drops to nearly zero (0.05 eV) by the $(5a, 4z)$. From DFT calculations, there is no clear consensus on the spin multiplicity of the acenes beyond octacene. Houk et al. [31] and Rayne et al. [32] show that nonacene is a triplet, while Bendikov et al. [10] report a singlet state, at least through decacene. Going beyond DFT, Casanova and Head-Gordon [23] developed a single-reference (5A_1) spin-flip configuration interaction method that predicts a singlet up to 20-acene, though the S-T splitting is nearly zero (0.09 eV). MR-CISD was used recently with an S-T splitting for decacene (Table 3 in Ref. [33]) consistent with our MR-CISD values (Fig. 4, Table S3). DMRG calculations [19] have been interpreted to result in a small but finite singlet–triplet gap. Hajgató et al. [25] concluded that the S-T splitting in the large n limit would be around 0.17 eV and went later on [24] to show with single-reference CCSD(T) that this limit is ~ 0.06 eV. Their study included up to $n = 11$ in the acene series and gave an S-T splitting for $n = 11$ of 0.31 eV. This value falls within the same near-degeneracy that our adjusted MR-AQCC predicts. To our knowledge, there is no current experimental S-T data for the periacene series. Additionally, we have only found one other group [60] that reported theoretical S-T data for periacenes. With R(U)B3LYP/3-21G, they found a -0.33 eV S-T splitting for the $(5a, 5z)$ periacene, indicating a triplet ground state. For the MR-AQCC/CAS(8,8)/6-31G calculation, we find a splitting of 0.05 eV. Accordingly, all these calculations strongly suggest that an actual graphene nanoribbon has a ground state with nearly degenerate singlet and triplet states.

The comparison between the basis sets (6-31G and 6-31G*) and the two different electronic systems (π -conjugated and total) for the linear acenes, as shown in Fig. 6 (Table S5), leads to the conclusion that the π -conjugated system with a 6-31G basis set is quite adequate to describe the S-T splitting for these molecules. There is virtually no

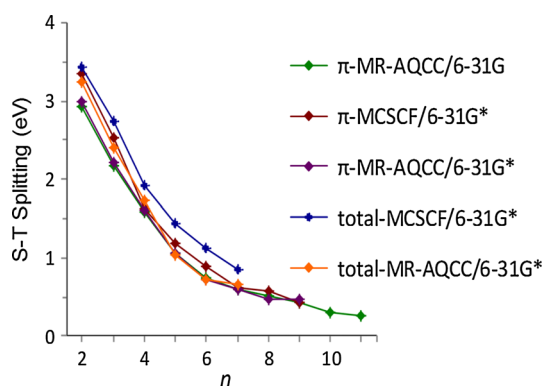


Fig. 6 Singlet–triplet splitting for the n -acenes computed at MCSCF and MR-AQCC levels for three different cases: π -6-31G, π -6-31G*, and total-6-31G*

difference in the relative S-T splittings for the three MR-AQCC variants. This is true in particular for the larger systems beyond pentacene where the three values are always within an interval of 0.1 eV. Only the S-T splittings computed at the MCSCF level deviate a bit from the MR-AQCC results. Also, what can be seen from these graphs is that a systematic error with respect to experiment, as shown in Table 1, still arises in the MR-AQCC, regardless of the basis or level of σ - π correlation. Thus, it is not the freezing of the σ orbitals that leads to the error, and accordingly, the SCF approach seems to be sufficient for the description of the σ system. While the MR-AQCC corrects for the size extensivity issue present in MR-CISD, it is likely the truncated nature of the calculations that still causes this error.

3.2 Radical character

It is primarily the zigzag edge of graphene nanoribbons that contributes to its high radical character. Nakada et al. [61] showed analytically that there is a degenerate flat band near the Fermi level on the zigzag edge, which is not present on the armchair edge. Jiang et al. [15] went on to show that the carbon atoms on the zigzag edge of a graphene nanoribbon are more chemically reactive than those of a graphene sheet, nanotube, and nanoribbon armchair edge, having a bond dissociation energy at least 1.2 eV times higher than any of them when bonded to hydrogen. The radical character of the system is examined via two means in this paper: the NO occupation and effective number of unpaired electrons.

3.2.1 NO occupation

The NO occupations are derived from the spin-averaged one-electron density matrix, thus leading to a spectrum of occupation from zero to two. This can be seen for the $^3B_{3u}$

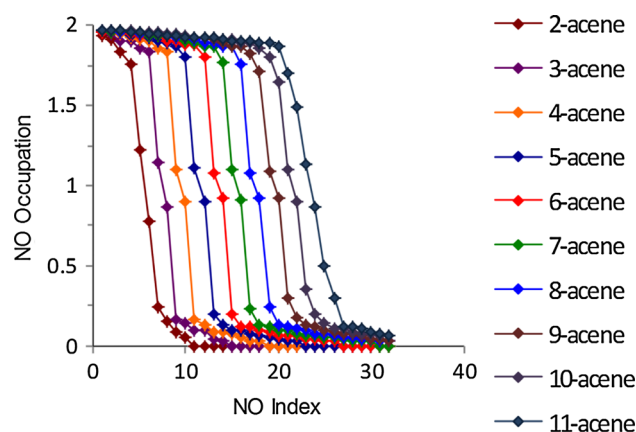


Fig. 7 Natural orbital (NO) occupations of the $^3B_{3u}$ state of n -acenes ($n = 2$ –11) obtained from π -MR-AQCC/RAS/CAS(4,4)/AUX/6-31G calculations

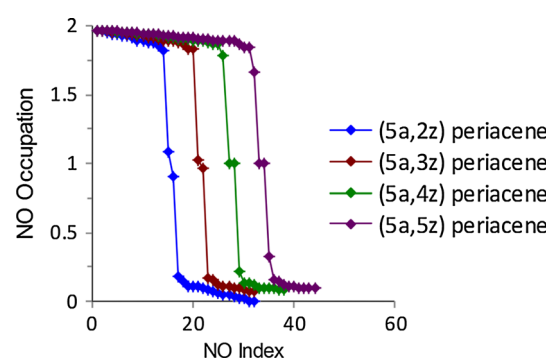


Fig. 8 Natural orbital (NO) occupations of the $^3B_{3u}$ state of ($5a,nz$) periacenes ($n = 2$ –5) obtained from π -MR-AQCC/CAS(8,8)/6-31G calculations

state for the acenes in Fig. 7 and for the $^3B_{3u}$ state for the periacenes in Fig. 8. The HONO and LUNO for each molecule can be recognized by the occupations closest to one for the whole series. The acene series starts for $n = 2$ with a HONO/LUNO difference of about 0.56, which is reduced to about 0.27. With increasing n , additional NO occupations deviating from the limit values of zero and two appear, indicating the evolving polyradical character. This evolution of increasing radical character is analogous to the one found for the lowest singlet state of acenes in the MR-AQCC [26], DMRG [19], 2-RDM [21], and projected Hartree–Fock calculations [12]. DMRG calculations on larger acenes [20] show for the singlet state a HONO/LUNO gap of $\sim 0.5e$, which is classified by the authors as single radical occupation being, in their conclusions, similar to the just-mentioned other calculations. The singlet and triplet NO occupation plots differ primarily for the initial members of the acene series, which starts with HONO/LUNO occupations for the singlet case close to

zero and two, respectively, whereas in the triplet case, the aforementioned open-shell NOs already appear at the very beginning of the series. However, after a certain size of the

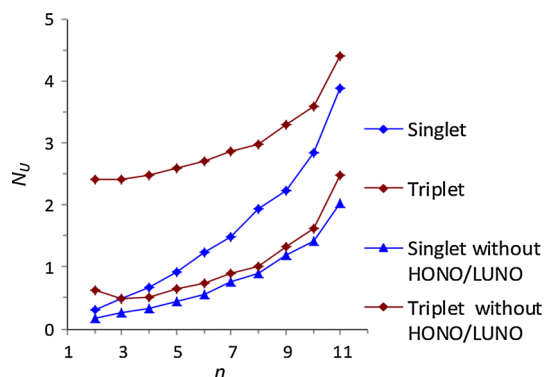


Fig. 9 Effective number of unpaired electrons for the 1A_g and $^3B_{3u}$ states of the n -acenes with and without the HONO and LUNO included using the π -MR-AQCC/RAS/CAS(4,4)/AUX/6-31G method

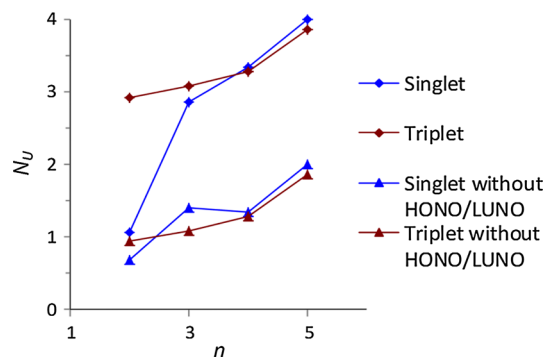
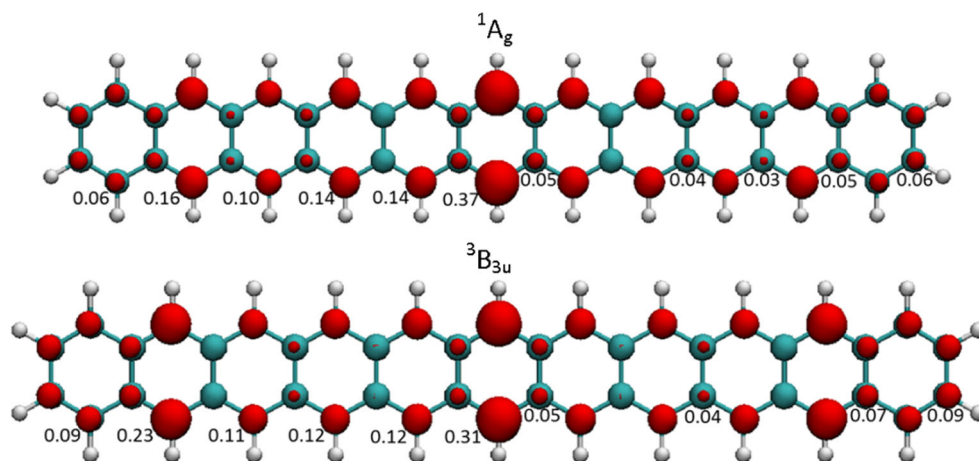


Fig. 10 Effective number of unpaired electrons for the 1A_g and $^3B_{3u}$ states of the $(5a,nz)$ periacene series with and without the HONO and LUNO included using the π -MR-AQCC/CAS(8,8)/6-31G method

Fig. 11 Unpaired electron density for the 1A_g (top) and $^3B_{3u}$ (bottom) states of the 11-acene (isovalue 0.005 a.u.) of the π -MR-AQCC/RAS(6)/CAS(4,4)/AUX(6)/6-31G calculation with individual atomic populations computed from a Mulliken analysis



acene chain, the NO occupation graphs look very similar. The same situation is seen with the periacenes in Fig. 3 of Ref. [26] and Fig. 8. HONO/LUNO plots for the 11-acene and $(5a,5z)$ periacene for both the 1A_g and $^3B_{3u}$ states are included in the supplementary material (Figures S1–4).

3.2.2 Effective number of unpaired electrons

In Fig. 9, the N_U values (Eq. 2) for the singlet and triplet states of the acene series are presented. The triplet curve starts from a value of 2.4 for $n = 2$, which is consistent with the strong open-shell character shown in Fig. 7. The singlet state starts with closed-shell character, but then, it rapidly catches up with the triplet state. It has been found for a true biradical (the stacked tetracyanoethylene anion dimer complex with two potassium cations as counter ions) [62] that the N_U values could be modeled by the HONO/LUNO contributions alone. The situation is completely different here. There is still a strong increase in N_U even after the HONO/LUNO contribution is deducted (Fig. 9). A similar situation is found for the periacenes (Fig. 10). It is interesting to note that the partial number of unpaired electrons is almost identical for the singlet and triplet states in all cases considered. This suggests similarities between the many-particle wave functions in both cases and that the single major difference lies in the frontier orbitals, which are only in the triplet case necessarily occupied by unpaired electrons. As soon as the singlet acquires radical character its total N_U reaches the value of the triplets. Plots of the unpaired densities including a Mulliken population analysis are given in Figs. 11 and 12. The unpaired density is always located on the zigzag edge. There is a specific concentration on the center, but a delocalization over the whole edge is visible.

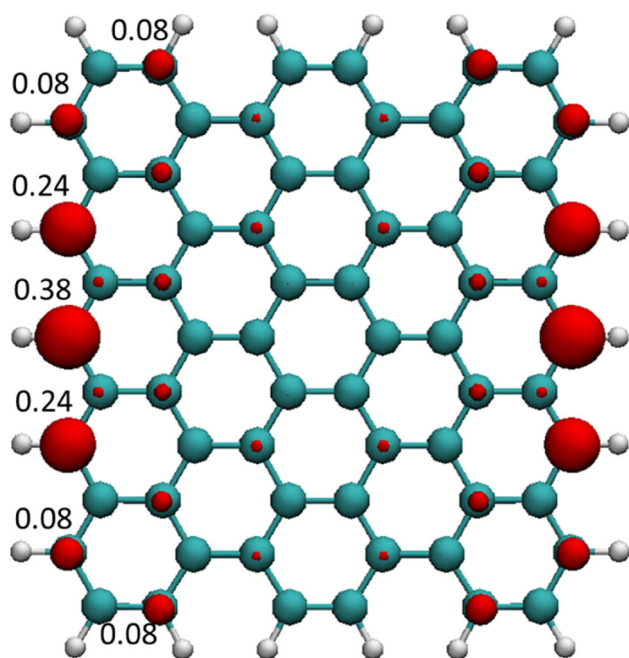


Fig. 12 Unpaired electron density for the ${}^3B_{3u}$ state of the $(5a,5z)$ periacene (isovalue 0.005 a.u.) of the π -MR-AQCC/CAS(8,8)/6-31G calculation with individual atomic populations computed from a Mulliken analysis

4 Conclusions

The purpose of this work was twofold: first, to determine whether the ground state of graphene nanoribbons is a singlet or a triplet and second, to qualify/quantify the multiradical nature of these systems. This was accomplished by performing high-level ab initio multiconfigurational and multireference calculations using the COLUMBUS program on quasi-linear acenes and two-dimensional periacenes. It is clearly seen that the validity of the results of these calculations is independent of both the basis set and the amount of correlated σ electrons. For both systems, a near-degeneracy of the singlet and triplet states is found for sufficiently extended systems. For the n -acene series, this happens at around $n = 11$. In particular, in the periacene case, the S-T splitting drops rapidly to nearly zero eV by the $(5a,4z)$. It is clear, however, from the calculations that graphene is multiradical in nature as the number of unpaired electrons increases with chain length. As in the case of the singlet state, the unpaired densities in the periacenes are concentrated along the zigzag edges with only minor extension into the inner parts of the nanosheet. The multiradical character of the acenes and periacenes leads to very high reactivity, which will be amenable to tuning, either by structural defects or by heteroatoms. Further work will examine various forms of defects in regard to their stability and electronic properties.

Acknowledgments This work was supported by the National Science Foundation under Project No. CHE-1213263, by the Austrian Science Fund (SFB F41, ViCoM, and Project P20893-N19), and the Robert A. Welch Foundation under Grant No. D-0005. Shawn Horn is funded by a research fellowship at Texas Tech University. Computer time at the Vienna Scientific Cluster (Project Nos. 70151 and 70376) and by the Chemistry Computational Cluster of Texas Tech University is gratefully acknowledged.

References

- Geim A, Novoselov K (2007) Nat Mater 6:183
- Bendikov M, Wudl F, Perepichka D (2004) Chem Rev 104:4891
- Novoselov K, Jiang D, Schedin F, Booth T, Khotkevich V, Morozov S, Geim A (2005) Proc Natl Acad Sci 102:10451
- Lu G, Yu K, Wen Z, Chen J (2013) Nanoscale 5:1353
- Son Y, Cohen M, Louie S (2006) Nature 444:347
- Angliker H, Rommel E, Wirz J (1982) Chem Phys Lett 87:208
- Mondal R, Shah B, Neckers D (2006) J Am Chem Soc 128:9612
- Tonshoff C, Bettinger H (2010) Angew Chem Int Ed 49:4125
- Zade SS, Bendikov M (2010) Angew Chem Int Edit 49:4012
- Bendikov M, Duong H, Starkey K, Houk K, Carter E, Wudl F (2004) J Am Chem Soc 126:7416
- Jiang D, Dai S (2008) J Phys Chem A 112:332
- Rivero P, Jimenez-Hoyos C, Scuseria G (2013) J Phys Chem B 117:12750
- Zimmerman P, Bell F, Casanova D, Head-Gordon M (2011) J Am Chem Soc 133:19944
- Hod O, Barone V, Scuseria G (2008) Chem Phys Lett 466:72
- Jiang D, Sumpter B, Dai S (2007) J Chem Phys 126:134701
- Nagai H, Nakano M, Yoneda K, Kishi R, Takahashi H, Shimizu A, Kubo T, Kamada K, Ohta K, Botek E, Champagne B (2010) Chem Phys Lett 489:212
- Barone V, Hod O, Peralta J, Scuseria G (2011) Acc Chem Res 44:269
- Jiang DE, Dai S (2008) Chem Phys Lett 466:72
- Hachmann J, Dorando J, Aviles M, Chan G (2007) J Chem Phys 127:134309
- Mizukami W, Kurashige Y, Yanai T (2012) J Chem Theory Comput 9:401–407
- Gidofalvi G, Mazziotti D (2008) J Chem Phys 129:134108
- Pelzer K, Greenman L, Gidofalvi G, Mazziotti D (2011) J Phys Chem A 115:5632
- Casanova D, Head-Gordon M (2009) Phys Chem Chem Phys 11:9779
- Hajgato B, Huzak M, Deleuze M (2011) J Phys Chem A 115:9282
- Hajgato B, Szieberth D, Geerlings P, de Proft F, Deleuze M (2009) J Chem Phys 131:22
- Plasser F, Pasalic H, Gerzabek M, Libisch F, Reiter R, Burgdorfer J, Muller T, Shepard R, Lischka H (2013) Angew Chem Int Ed 52:2581
- Wassmann T, Seitsonen AP, Saitta AM, Lazzeri M, Mauri F (2010) J Am Chem Soc 132:3440
- Balaban AT, Klein DJ (2009) J Phys Chem C 113:19123
- Pisani L, Chan JA, Montanari B, Harrison NM (2007) Phys Rev B 75:064418
- Purushotharman B, Bruzek M, Parkin S, Miller A, Anthony J (2011) Angew Chem Int Ed 50:7013
- Houk K, Lee P, Nendel M (2001) J Org Chem 66:5517
- Rayne S, Forest K (2011) Comput Theor Chem 976:105
- Chakraborty H, Shukla A (2013) J Phys Chem A 117:14220
- Knippenberg S, Starcke JH, Wormit M, Dreuw A (2010) Mol Phys 108:2801

35. Szalay P, Bartlett R (1993) *Chem Phys Lett* 214:481
36. Antol I, Eckert-Maksic M, Lischka H, and Maksic Z (2007) *Eur J Org Chem* 3173
37. Wang E, Parish C, Lischka H (2008) *J Chem Phys* 129:044306
38. Szalay P, Muller T, Gidofalvi G, Lischka H, Shepard R (2012) *Chem Rev* 112:108
39. Takatsuka K, Fueno T, Yamaguchi K (1978) *Theor Chim Acta* 48:175
40. Staroverov V, Davidson E (2000) *Chem Phys Lett* 330:161
41. Head-Gordon M (2003) *Chem Phys Lett* 372:508
42. Moller C, Plesset M (1934) *Phys Rev* 46:0618
43. Vahtras O, Almlöf J, Feyereisen M (1993) *Chem Phys Lett* 213:514
44. Weigend F, Häser M (1997) *Theor Chem Acc* 97:331
45. Schafer A, Horn H, Ahlrichs R (1997) *J Chem Phys* 97:2571
46. Luken W (1978) *Chem Phys Lett* 58:421
47. Hehre W, Ditchfield R, Pople J (1972) *J Chem Phys* 56:2257
48. Hosteny R, Dunning T Jr, Gilman R, Pipano A, Shavitt I (1975) *J Chem Phys* 62:4764
49. Becke A (1988) *Phys Rev A* 38:3098
50. Perdew J (1986) *Phys Rev B* 33:8822
51. Häser M, Ahlrichs R (1989) *J Comput Chem* 10:104
52. Treutler O, Ahlrichs R (1995) *J Chem Phys* 102:346
53. Lischka H, Shepard R, Pitzer R, Shavitt I, Dallos M, Muller T, Szalay P, Seth M, Kedziora G, Yabushita S, Zhang Z (2001) *Phys Chem Chem Phys* 3:664
54. Lischka H, Shepard R, Shavitt I, Pitzer R, Dallos M, Müller T, Szalay P, Brown F, Ahlrichs R, Böhm H, Chang A, Comeau D, Gdanitz R, Dachsel H, Ehrhardt C, Ernzerhof M, Höchtel P, Irle S, G K, Kovar T, Parasuk V, Pepper M, Scharf P, Schiffer H, Schindler M, Schüler M, Seth M, Stahlberg E, Zhao J-G, Yabushita S, Z Z, Barbatti M, Matsika S, Schuurmann M, Yarkony D, Brozell S, Beck E, Blaudeau J-P, Ruckebauer M, Sellner B, Plasser F, Szymczak J (2012) COLUMBUS, an ab initio electronic structure program, release 7.0
55. Lischka H, Muller T, Szalay PG, Shavitt I, Pitzer RM, Shepard R (2011) *Wires Comput Mol Sci* 1:191
56. Birks J (1970) *Photophysics of aromatic molecules*. Wiley, London
57. Schiedt J, Weinkauff R (1997) *Chem Phys Lett* 266:201
58. Sabbatini N, Indelli M, Gandolfi M, Balzani V (1982) *J Phys Chem* 86:3585
59. Burgos J, Pope M, Swendberg C, Alfano R (1977) *Phys Status Solidi B* 83:249
60. Wang J, Zubarev D, Philpott M, Vukovic S, Lester W, Cui T, Kawazoe Y (2010) *Phys Chem Chem Phys* 12:9839–9844
61. Nakada K, Fujita M, Dresselhaus G, Dresselhaus M (1996) *Phys Rev B* 54:17954
62. Cui Z, Lischka H, Mueller T, Plasser F, Kertesz M (2013) *Chem Phys Chem*. doi:10.1002/cphc.201300784